Simultaneous analysis of the Ballik-Ramsay and Phillips systems of C_2 and observation of forbidden transitions between singlet and triplet states

Wang Chen,[1] Kentarou Kawaguchi,[1] Peter F. Bernath,[2] and Jian Tang[1,a)]
[1]*Graduate School of Natural Science and Technology, Okayama University, 3-1-1 Tsushima-naka, Kita-ku, Okayama 700-8530, Japan*
[2]*Department of Chemistry and Biochemistry, Old Dominion University, 4541 Hampton Boulevard, Norfolk, Virginia 23529-0126, USA*

(Received 1 December 2014; accepted 23 January 2015; published online 13 February 2015)

6229 lines of the Ballik-Ramsay system ($b^3\Sigma_g^- – a^3\Pi_u$) and the Phillips system ($A^1\Pi_u – X^1\Sigma_g^+$) of C_2 up to v = 8 and J = 76, which were taken from the literature or assigned in the present work, were analyzed simultaneously by least-squares fitting with 82 Dunham-like molecular parameters and spin-orbit interaction constants between the $b^3\Sigma_g^-$ and $X^1\Sigma_g^+$ states with a standard deviation of 0.0037 cm^{-1} for the whole data set. As a result of the deperturbation analysis, the spin-orbit interaction constant A_{bX} was determined as 6.333(7) cm^{-1} and the energy difference between the $X^1\Sigma_g^+$ and $a^3\Pi_u$ states was determined as 720.008(2) cm^{-1} for the potential minima or 613.650(3) cm^{-1} for the v = 0 levels with Merer and Brown's N^2 Hamiltonian for $^3\Pi$ states, which is about 3.3 cm^{-1} larger than the previously determined value. Due to this sizable change, a new energy-level crossing was found at J = 2 for v = 3 (F_1) of $b^3\Sigma_g^-$ state and v = 6 of $X^1\Sigma_g^+$ state, where the strong interaction causes a nearly complete mixing of the wave functions of the $b^3\Sigma_g^-$ and $X^1\Sigma_g^+$ states and the forbidden transitions become observable. Using the predictions of our deperturbation analysis, we were able to identify 16 forbidden transitions between the singlet and triplet states at the predicted frequencies with the expected intensities, which verifies our value for the energy difference between the $X^1\Sigma_g^+$ and $a^3\Pi_u$ states. © *2015 AIP Publishing LLC.* [http://dx.doi.org/10.1063/1.4907530]

I. INTRODUCTION

C_2 is ubiquitous in astronomical environments, flames, and carbon plasmas used to make nanostructures.[1] Due to the presence of many low-lying electronic states in C_2, various vibronic band systems, such as the Swan system ($d^3\Pi_g – a^3\Pi_u$), the Phillips system ($A^1\Pi_u – X^1\Sigma_g^+$), and the Ballik-Ramsay system ($b^3\Sigma_g^- – a^3\Pi_u$), have been observed in the visible and infrared regions and studied extensively for a long time.[2]

The congestion of the vibronic states in C_2, as shown in Fig. 1, often causes perturbations in the observed spectra due to interactions between the accidentally crossing rotational levels. These perturbations provide information on the energy difference between electronic states with different multiplicities and sometimes even locate unknown or dark electronic states. Historically, the perturbations observed for the Phillips system and the Ballik-Ramsay system were found to be due to the spin-orbit interaction between the $X^1\Sigma_g^+$ and $b^3\Sigma_g^-$ states,[3] and a deperturbation analysis located the $a^3\Pi_u$ state 610 ± 5 cm^{-1} above the $X^1\Sigma_g^+$ ground state for the v = 0 vibrational energy levels,[4] or 716.24 ± 5 cm^{-1} for the potential minima of the two electronic states.[5] The small perturbations observed in the upper $A^1\Pi_u$ state of the Phillips system also led to the prediction of a dark $c^3\Sigma_u^+$ state.[5–7] Finally, in 2006, Kokkin *et al.*[8] successfully observed the new $d^3\Pi_g – c^3\Sigma_u^+$ system by laser-induced fluorescence (LIF) spectroscopy.[9] Interestingly, Nakajima and Endo[10] carried out a recent deperturbation analysis for the $c^3\Sigma_u^+$, $a^3\Pi_u$, and $A^1\Pi_u$ states for their observed LIF spectrum of the $d^3\Pi_g – c^3\Sigma_u^+$ system and the Swan system, which indicated that there are no significant level shifts caused by the spin-orbit interaction between v = 2 of $A^1\Pi_u$ and v = 1(F_2) of $c^3\Sigma_u^+$. The small perturbations observed previously for J = 19 and 21 of $A^1\Pi_u$ (v = 2) of the Phillips system, which led to the well-known prediction of the $c^3\Sigma_u^+$ dark state, are in fact due to the interaction between v = 2 of $A^1\Pi_u$ and v = 7(F_2) of $a^3\Pi_u$. As another example, many perturbations for the upper $d^3\Pi_g$ state of the Swan system were attributed to vibronic interactions with two unknown $B^1\Delta_g$ and $B'^1\Sigma_g^+$ states and high vibrational levels of the $b^3\Sigma_g^-$ and $X^1\Sigma_g^+$ states.[11] Later in 1988, Bernath and coworkers observed the $B^1\Delta_g – A^1\Pi_u$ and $B'^1\Sigma_g^+ – A^1\Pi_u$ systems in the infrared region.[12] The abnormal intensity enhancement observed in the Swan system for the $d^3\Pi_g$, v = 6 vibrational level (the so called high pressure bands) was proposed to be caused by the perturbation of an unknown $1^5\Pi_g$ dark state.[13] In 2011, Bornhauser *et al.*[14] observed the forbidden transitions between the $1^5\Pi_g$ and $a^3\Pi_u$ states due to the vibronic mixing of $d^3\Pi_g$ and $1^5\Pi_g$ by double-resonance four-wave mixing spectroscopy and accurately determined the energy difference between the $1^5\Pi_g$ and $a^3\Pi_u$ states as 29 258.592(5) cm^{-1}. In contrast, the energy difference between the $a^3\Pi_u$ and $X^1\Sigma_g^+$ states has not been determined directly by observing forbidden transitions between the singlet and triplet states of C_2.

The initial deperturbation analysis by Ballik and Ramsay[3–5] for the interaction between the $X^1\Sigma_g^+$ and $b^3\Sigma_g^-$

a)Author to whom correspondence should be addressed. Electronic mail: jtang@okayama-u.ac.jp

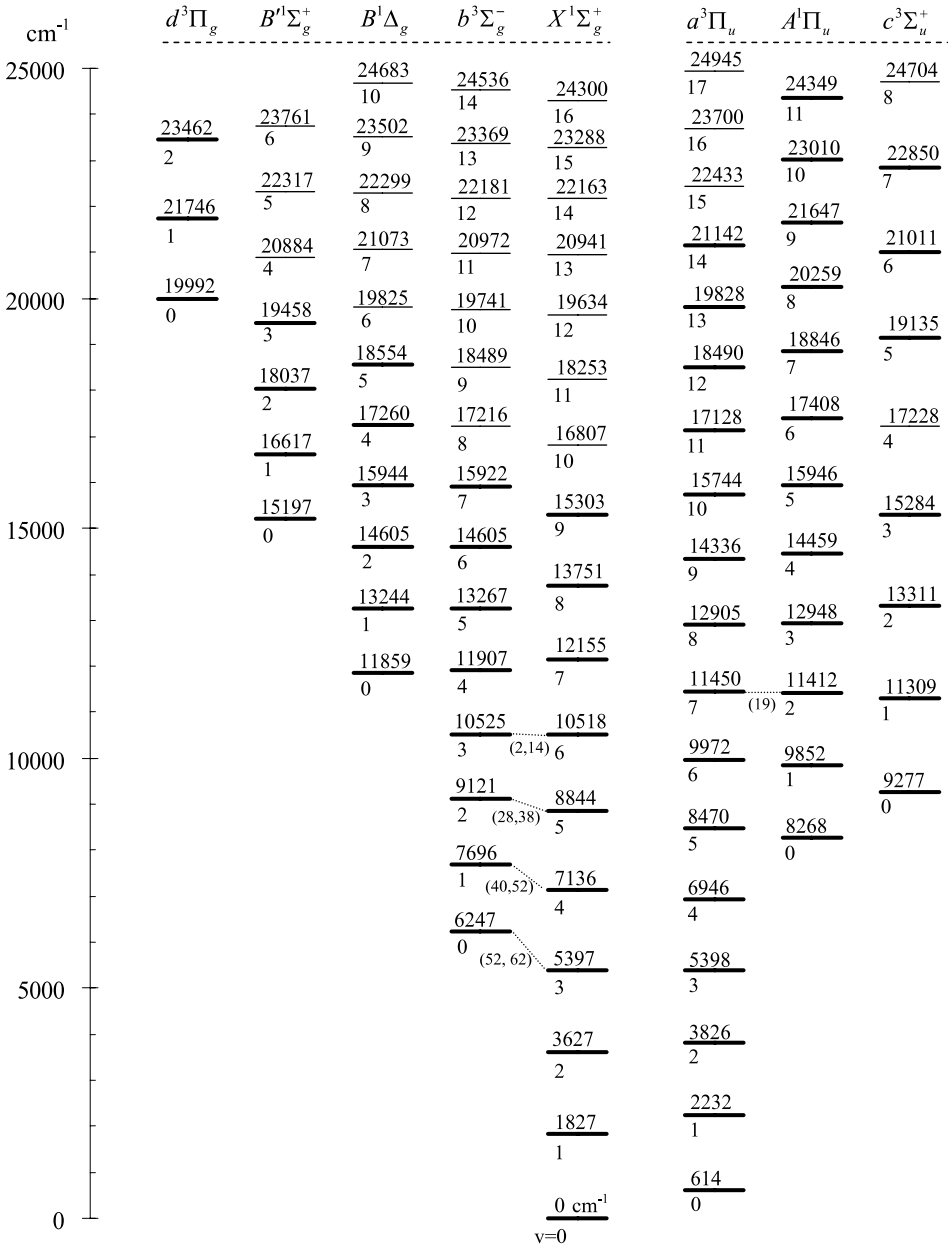

FIG. 1. Vibronic energy levels of C_2 below 25 000 cm^{-1}. The levels which have been observed so far are drawn with bold lines. The values below the levels are the vibrational quantum numbers, and the upper values are term energies T_v in cm^{-1} relative to the vibrational level v = 0 of $X^1\Sigma_g^+$, which are from Ref. 19 ($X^1\Sigma_g^+$ and $A^1\Pi_u$), Ref. 28 ($a^3\Pi_u$ and $d^3\Pi_g$), Ref. 15 ($b^3\Sigma_g^-$), Ref. 12 ($B^1\Delta_g$ and $B'^1\Sigma_g^+$), and Ref. 29 ($c^3\Sigma_u^+$ and many higher v states of the other electronic states). The singlet-triplet gap between v = 0 of $X^1\Sigma_g^+$ and $a^3\Pi_u$ is taken as 613.650(3) cm^{-1} from the present study. The dashed lines between the levels indicate that perturbations near the level crossing have been observed, and the values within the brackets are the J-values at the level crossings. The level crossing at $J = 2$ of $b^3\Sigma_g^-$ v = 3 (F_1) and $X^1\Sigma_g^+$ v = 6 was found in the present study.

states was carried out for 9 emission bands of the Ballik-Ramsay system involving levels of the $b^3\Sigma_g^-$ state up to v = 4, which were observed by a vacuum infrared grating spectrometer with a spectral resolution of 0.01-0.05 cm^{-1} and absolute accuracy of around 0.05 cm^{-1}. Later, Amiot *et al.*[15] observed 14 emission bands of the Ballik-Ramsay system involving levels of the $b^3\Sigma_g^-$ state up to v = 7 with a Fourier transform infrared (FTIR) spectrometer with a resolution of 0.028 cm^{-1}, and their deperturbation analysis resulted in an energy difference of ΔE ($a^3\Pi_u$–$X^1\Sigma_g^+$) = 718.32 cm^{-1} in comparison with the previous value of 716.24 cm^{-1}. Roux *et al.*[16] then carried out a new FTIR measurement with a resolution of 0.013 cm^{-1} and corrected many errors in the previous assignment[15] of the Ballik-Ramsay system near the perturbation. As a result, the deperturbation analysis for the spin-orbit interaction constants between the $X^1\Sigma_g^+$ and $b^3\Sigma_g^-$ states was improved by the inclusion of a higher-order term.[16] In all these previous analyses, effective molecular constants for each vibrational level were determined first with the "unperturbed" transitions of the Ballik-Ramsay system, and the deperturbation was carried out by analyzing the shifts of the "perturbed" transition frequencies from the values calculated with the effective molecular constants obtained from the "unperturbed" transitions. Then, a Dunham-like vibrational expansion of the molecular constants was obtained by analysis of the effective molecular constants for the various vibrational levels, and the energy difference and the spin-orbit interaction constants between the $X^1\Sigma_g^+$ and $b^3\Sigma_g^-$ states were derived by a deperturbation analysis. These analyses have omitted the vibronic interaction for the "unperturbed" transitions near the "perturbed" transitions, which means that the effective molecular constants for the "unperturbed" transitions are, in fact, affected partly by the background-like vibronic interactions. In addition, the derived energy difference and the spin-orbit interaction constants are also affected by the incomplete shift of the "perturbed" transition frequencies. In other words, these previous analyses are only a partial deperturbation.

In the analysis of the pure rotational transitions of MgO within the $X^1\Sigma$ and $a^3\Pi$ states,[17] a simultaneous deperturbation for all the transitions involving the $X^1\Sigma$, $a^3\Pi$, and $A^1\Pi$ states was successful by fitting a set of molecular constants with vibrational expansions, the spin-orbit interaction between $X^1\Sigma$ and $a^3\Pi$, and the orbit-rotation interaction between $X^1\Sigma$ and $A^1\Pi$ and by using calculated vibrational overlap integrals and $\langle v_A|B(r)|v_X\rangle$. In a similar analysis, in the present study, we analyzed all the transitions ("perturbed" and "unperturbed") simultaneously for the Phillips system and the Ballik-Ramsay system of C_2 directly using Dunham-like molecular constants with vibrational expansions. The more complete deperturbation for C_2 resulted in a new energy difference of ΔE ($a^3\Pi_u$–$X^1\Sigma_g{}^+$) = 721.640 (2) cm^{-1}, a change of 3.3 cm^{-1} from the previous value, which led to the discovery of a new level-crossing with a very strong perturbation. Eventually, the forbidden transitions between the singlet and triplet electronic states were found at this level crossing, which in turn confirmed our new value of the singlet-triplet energy difference.

II. DATA SET FOR ANALYSIS

The data used for the present analysis, about 6229 lines (16 lines due to forbidden transitions are included), were partly taken from previous studies and partly assigned in this work, as summarized in Table I. For the 4878 transitions of the Ballik-Ramsay system, we took 1294 lines from the FTIR spectrum of Roux *et al.*[16] with a spectral resolution of 0.013 cm^{-1}, 527 lines from the FTIR spectrum of Amiot *et al.*[15] with a spectral resolution of 0.028 cm^{-1}, and 112 lines of satellite branches for the v′-v″ = 0-0 band of the Ballik-Ramsay system with interconnections between the different F levels from the FTIR spectrum of Davis *et al.*[18] with a spectral resolution of 0.015 cm^{-1}. For the 1335 transitions of the Phillips system, we took 500 lines from the FTIR spectrum of Douay *et al.*[19] with a spectral resolution of 0.013 cm^{-1}, 283 lines from the laser absorption spectrum of Chan *et al.*[20] with a spectral resolution of 0.013 cm^{-1}, and 145 lines from the FTIR spectrum of Chauville *et al.*[6] with a spectral resolution of 0.026-0.040 cm^{-1}. In the present work, we assigned the rest of 3368 lines for 11 bands of the Phillips system and 12 bands of the Ballik-Ramsay system, as shown in Table I, and the satellite branches for the v′-v″ = 1-0, 2-1, 3-2, 0-1, 1-2, 2-3, and 3-4 bands of the Ballik-Ramsay system with interconnections between the different F levels from the FTIR spectrum of Ghosh *et al.*[21] with a spectral resolution of 0.02 cm^{-1} and from the FTIR spectrum of Douay *et al.*[19] Previously, Yan *et al.* observed the v′-v″ = 0-1, 1-2, 2-3 bands of the Ballik-Ramsay system by laser spectroscopy with magnetic rotation.[22] The bands associated with v = 4 of $a^3\Pi$ are mostly assigned in our present analysis. The complete line list used is available online as supplementary material.[23] We have also assigned several bands associated with v = 5 and 6 of $a^3\Pi$ as shown in the supplementary material, but they were not included in the present deperturbation analysis due to some new perturbations other than the ones considered in this work, which may be caused by the interactions with the $c^3\Sigma_u{}^+$ state. The deperturbation analysis is still under way for a future publication.

III. DEPERTURBATION ANALYSIS

The standard energy level expressions for the $X^1\Sigma_g{}^+$ and $A^1\Pi_u$ states are

$$E(X^1\Sigma_g{}^+) = G_v + B_v x - D_v x^2,$$
$$E(A^1\Pi_u) = T_e + G_v + B_v(x-1) - D_v(x-1)^2 \pm \tfrac{1}{2}\left(q_v x + q_D x^2\right),$$

in which T_e is the electronic energy, $x = J(J+1)$, and

$$G_v = \omega_e\left(v+\tfrac{1}{2}\right) - \omega_e x_e\left(v+\tfrac{1}{2}\right)^2 + \omega_e y_e\left(v+\tfrac{1}{2}\right)^3 + \omega_e z_e\left(v+\tfrac{1}{2}\right)^4 + \omega_e a_e\left(v+\tfrac{1}{2}\right)^5,$$

TABLE I. C_2 bands used in the present analysis.

	Δv	v′-v″ (J_{max})						
Phillips $A^1\Pi_u$–$X^1\Sigma_g{}^+$	−3	0-3 (22)[a]	1-4 (22)[a]	2-5 (22)[a]	3-6 (20)[a]			
	−2	0-2 (34)[b]	1-3 (32)[b]	2-4 (38)[b]	3-5 (28)[b]	4-6 (20)[b]		
	−1	0-1 (40)[b]	1-2 (36)[b]	2-3 (36)[b]	3-4 (22)[a]			
	0	0-0 (52)[b]	1-1 (20)[a]	2-2 (36)[a]	3-3 (40)[b]	4-4 (32)[b]	5-5 (22)[b]	6-6(10)[a]
	1	1-0 (30)[c]	2-1 (44)[c]	5-4 (20)[a]	6-5 (18)[a]	7-6 (22)[a]		
	2	2-0 (20)[d]	3-1 (20)[d]	4-2 (18)[d]				
	3	3-0 (22)[d]	4-1 (18)[d]	5-2 (18)[d]	6-3 (16)[d]			
	4	5-1 (20)[d]	6-2 (18)[d]	7-3 (18)[d]	8-4 (18)[d]			
Ballik-Ramsay $b^3\Sigma_g{}^-$–$a^3\Pi_u$	−2	0-2 (25)[a]	1-3 (30)[a]	2-4 (21)[a]				
	−1	0-1 (39)[a]	1-2 (37)[a]	2-3 (35)[a]	3-4 (35)[a]			
	0	0-0 (76)[e]	1-1 (62)[e]	2-2 (27)[a]	4-4 (27)[a]			
	1	1-0 (66)[e]	2-1 (64)[e]	3-2 (60)[e]	4-3 (38)[a]	5-4 (30)[a]		
	2	2-0 (60)[e]	3-1 (62)[e]	4-2 (61)[e]	5-3 (55)[e]	6-4 (39)[a]		
	3	3-0 (48)[f]	4-1 (56)[f]	5-2 (42)[f]	6-3 (58)[f]	7-4 (39)[f]		

[a]Present work.
[b]Douay *et al.* (Ref. 19).
[c]Chauville *et al.* (Ref. 6).
[d]Chan *et al.* (Ref. 20).
[e]Roux *et al.* (Ref. 16).
[f]Amiot *et al.* (Ref. 15).

$$
\begin{aligned}
B_{\mathrm{v}} &= B_e - \alpha_e\left(\mathrm{v}+\tfrac{1}{2}\right) + \gamma_e\left(\mathrm{v}+\tfrac{1}{2}\right)^2 \\
&\quad + \delta_e\left(\mathrm{v}+\tfrac{1}{2}\right)^3 + \varepsilon_e\left(\mathrm{v}+\tfrac{1}{2}\right)^4, \\
D_{\mathrm{v}} &= D_e + \beta_e\left(\mathrm{v}+\tfrac{1}{2}\right) + \zeta_e\left(\mathrm{v}+\tfrac{1}{2}\right)^2, \\
q_{\mathrm{v}} &= q + \alpha^q\left(\mathrm{v}+\tfrac{1}{2}\right).
\end{aligned}
$$

The matrix elements of the effective N^2 Hamiltonian for the $a^3\Pi_u$ and $b^3\Sigma_g^-$ states using Hund's case (a) basis functions $0 = \left|{}^3\Pi_0\right\rangle$, $1 = \left|{}^3\Pi_1\right\rangle$, $2 = \left|{}^3\Pi_2\right\rangle$, $3 = \left|{}^3\Sigma_1^- e\right\rangle$, $4 = \left|{}^3\Sigma_0^- e\right\rangle$, and $5 = \left|{}^3\Sigma_1^- f\right\rangle$ are the same as those of Merer and Brown,[24] and Brazier *et al.*,[25]

$$
\begin{aligned}
H(0,0) &= T_e + G_{\mathrm{v}} - A_{\mathrm{v}} + \tfrac{2}{3}\lambda_{\mathrm{v}} + \left(B_{\mathrm{v}} - A_{D\mathrm{v}} + \tfrac{2}{3}\lambda_D\right)(x+2) - D_{\mathrm{v}}\left(x^2+6x+4\right) \\
&\quad + H_{\mathrm{v}}\left(x^3+12x^2+24x+8\right) \mp \left[o_{\mathrm{v}} + o_D(x+2) + p_{\mathrm{v}} + 2p_D(x+1) + q_{\mathrm{v}} + q_{D\mathrm{v}}(3x+2)\right], \\
H(1,1) &= T_e + G_{\mathrm{v}} - \tfrac{4}{3}\lambda_{\mathrm{v}} + \left(B_{\mathrm{v}} - \tfrac{4}{3}\lambda_D\right)(x+2) - D_{\mathrm{v}}\left(x^2+8x\right) + H_{\mathrm{v}}\left(x^3+18x^2+16x\right) \\
&\quad \mp \tfrac{1}{2}\left[2p_D x + q_{\mathrm{v}} x + q_{D\mathrm{v}} x(x+6)\right], \\
H(2,2) &= T_e + G_{\mathrm{v}} + A_{\mathrm{v}} + \tfrac{2}{3}\lambda_{\mathrm{v}} + \left(B_{\mathrm{v}} + A_{D\mathrm{v}} + \tfrac{2}{3}\lambda_D\right)(x-2) - D_{\mathrm{v}}\left(x^2-2x\right) + H_{\mathrm{v}}\left(x^3-4x\right), \\
H(0,1) &= -\sqrt{2x}\left\{B_{\mathrm{v}} - \tfrac{1}{2}A_{D\mathrm{v}} - \tfrac{1}{3}\lambda_D - 2D_{\mathrm{v}}(x+2) + H_{\mathrm{v}}\left(3x^2+16x+8\right)\right. \\
&\quad \left. \mp \tfrac{1}{2}\left[o_D + p_{\mathrm{v}} + p_D(x+3) + 2q_{\mathrm{v}} + q_{D\mathrm{v}}(3x+4)\right]\right\}, \\
H(0,2) &= -\sqrt{x(x-2)}\left\{2D_{\mathrm{v}} - H_{\mathrm{v}}(6x+4) \pm \tfrac{1}{2}\left[p_D + q_{\mathrm{v}} + q_{D\mathrm{v}}(x+2)\right]\right\}, \\
H(1,2) &= -\sqrt{2(x-2)}\left[B_{\mathrm{v}} + \tfrac{1}{2}A_{D\mathrm{v}} - \tfrac{1}{3}\lambda_D - 2D_{\mathrm{v}}x + H_{\mathrm{v}}\left(3x^2+4x\right) \mp \tfrac{1}{2}q_{D\mathrm{v}}x\right], \\
H(3,3) &= T_e + G_{\mathrm{v}} + B_{\mathrm{v}}x - D_{\mathrm{v}}\left(x^2+4x\right) + H_{\mathrm{v}}\left[x^3 + 4\left(3x^2+2x\right)\right] + \tfrac{2}{3}\lambda_{\mathrm{v}} + \tfrac{2}{3}\lambda_D x - \gamma_{\mathrm{v}} - 3\gamma_D x, \\
H(4,4) &= T_e + G_{\mathrm{v}} + B_{\mathrm{v}}(x+2) - D_{\mathrm{v}}\left(x^2+8x+4\right) + H_{\mathrm{v}}\left(x^3+18x^2+28x+8\right) \\
&\quad - \tfrac{4}{3}\lambda_{\mathrm{v}} - \tfrac{4}{3}\lambda_D(x+2) - 2\gamma_{\mathrm{v}} - 4\gamma_D(x+1), \\
H(5,5) &= T_e + G_{\mathrm{v}} + B_{\mathrm{v}}x - D_{\mathrm{v}}x^2 + H_{\mathrm{v}}x^3 + \tfrac{2}{3}\lambda_{\mathrm{v}} + \tfrac{2}{3}\lambda_D x - \gamma_{\mathrm{v}} - \gamma_D x, \\
H(3,4) &= -\tfrac{1}{2}(1 \pm 1)\sqrt{x}\left[2B_{\mathrm{v}} - 4D_{\mathrm{v}}(x+1) + H_{\mathrm{v}}\left(6x^2+20x+8\right) - \gamma_{\mathrm{v}} - \gamma_D(x+4)\right],
\end{aligned}
$$

where A is spin-obit constant, γ is spin-rotation constant, λ is spin-spin interaction constant, o, p, and q are Λ-type doubling constants, and H is a higher order centrifugal distortion constant. These parameters are further expanded by vibrational quantum number $(\mathrm{v}+1/2)$ as

$$
\begin{aligned}
H_{\mathrm{v}} &= H + \eta_e\left(\mathrm{v}+\tfrac{1}{2}\right), \\
A_{\mathrm{v}} &= A + \alpha^A\left(\mathrm{v}+\tfrac{1}{2}\right) + \gamma^A\left(\mathrm{v}+\tfrac{1}{2}\right)^2, \\
A_{D\mathrm{v}} &= A_D + \beta^{AD}\left(\mathrm{v}+\tfrac{1}{2}\right) + \zeta^{AD}\left(\mathrm{v}+\tfrac{1}{2}\right)^2, \\
\lambda_{\mathrm{v}} &= \lambda + \alpha^\lambda\left(\mathrm{v}+\tfrac{1}{2}\right), \\
\gamma_{\mathrm{v}} &= \gamma + \alpha^\gamma\left(\mathrm{v}+\tfrac{1}{2}\right) + \delta^\gamma\left(\mathrm{v}+\tfrac{1}{2}\right)^2, \\
o_{\mathrm{v}} &= o + \alpha^o\left(\mathrm{v}+\tfrac{1}{2}\right), \\
p_{\mathrm{v}} &= p + \alpha^p\left(\mathrm{v}+\tfrac{1}{2}\right) + \gamma^p\left(\mathrm{v}+\tfrac{1}{2}\right)^2, \\
q_{\mathrm{v}} &= q + \alpha^q\left(\mathrm{v}+\tfrac{1}{2}\right) + \gamma^q\left(\mathrm{v}+\tfrac{1}{2}\right)^2 + \delta^q\left(\mathrm{v}+\tfrac{1}{2}\right)^3, \\
q_{D\mathrm{v}} &= q_D + \beta^{qD}\left(\mathrm{v}+\tfrac{1}{2}\right) + \zeta^{qD}\left(\mathrm{v}+\tfrac{1}{2}\right)^2 + \theta^{qD}\left(\mathrm{v}+\tfrac{1}{2}\right)^3.
\end{aligned}
$$

The spin-orbit interaction between the $b^3\Sigma_g^-$ and $X^1\Sigma_g^+$ states is expressed as[16]

$$
\begin{aligned}
\left\langle {}^3\Sigma_{0e}^- \middle| \mathrm{H} \middle| {}^1\Sigma_{0e}^+ \right\rangle &= A + A_1(x+2) + A_2 x, \\
\left\langle {}^3\Sigma_{1e}^- \middle| \mathrm{H} \middle| {}^1\Sigma_{0e}^+ \right\rangle &= -2A_1\sqrt{x},
\end{aligned}
$$

where

$$
A = \left\langle b^3\Sigma_g^- \middle| H_{so} \middle| X^1\Sigma_g^+ \right\rangle = A_{bX}\langle \mathrm{v}_b | \mathrm{v}_X \rangle .
$$

$\langle \mathrm{v}_b | \mathrm{v}_X \rangle$ is an overlap integral and is calculated with Le Roy's "RKR" and "LEVEL" programs.[26] A_1 and A_2 represent effective second-order interaction constants. We set A_1 to a constant A_{bXD} in the analysis without considering A_2, which cannot be determined independently as shown in Ref. 16.

The least-squares fitting with 82 molecular constants was carried out simultaneously for the 6229 transitions of the Ballik-Ramsay system and the Phillips system with a standard deviation 0.0037 cm^{-1} for the residuals. The molecular constants obtained and a comparison with the previous work is shown in Table II.

In Amiot *et al.*'s analysis,[15] a different Hamiltonian for the $^3\Pi$ state (from Zare *et al.*[27] based on R^2) was used: the main difference is that the diagonal matrix elements are all one B_{v} constant smaller than for the N^2 Brown and Merer[24] Hamiltonian that we used. Since the resulting energy of the $^3\Pi$ state should be the same for both definitions, the one B_{v} difference in the expression for the diagonal matrix elements makes the T_e values differ by one B_{v} for the two definitions, that is, the T_e value for Zare *et al.*'s expression is one B_{v} constant (about 1.63 cm^{-1} for the $a^3\Pi_u$ state) larger than the value for Brown and Merer's expression, if higher-order terms are neglected. This also affects the values of other constants slightly: for example, the two definitions yield ω_e and $\omega_e x_e$ that differ by one α_e and one γ_e, respectively. For this reason, we have to be careful to use the same definition when we compare our T_e values for the $a^3\Pi_u$ state with Amiot *et al.*'s

TABLE II. Molecular constants determined by the simultaneous analysis (in cm^{-1}).

	$X^1\Sigma_g^+$				$A^1\Pi_u$		
	Present work	Douay *et al.*[19]	Chan *et al.*[20]		Present work	Douay *et al.*[19]	Chan *et al.*[20]
T_e	0	0	0	T_e	8391.406 2(19)	8393.408 5(46)	8393.414 8(29)
ω_e	1855.035 2(43)	1855.014(13)	1855.066 3(63)	ω_e	1608.217 8(25)	1608.199 0(52)	1608.231 7(38)
$\omega_e x_e$	13.570 1(36)	13.545(12)	13.600 7(54)	$\omega_e x_e$	12.078 6(17)	12.059 7(27)	12.084 8(25)
$\omega_e y_e$	−0.127 5(13)	−0.132 1(50)	−0.116 0(20)	$\omega_e y_e$	−0.003 71(49)	−0.010 555(39)	−0.002 88(72)
$\omega_e z_e$	0.003 13(20)	0.003 57(89)	0.001 260(32)	$\omega_e z_e$	−0.000 901(61)		−0.000 908(90)
$\omega_e a_e$	−0.001 112(11)	−0.001 116(57)	−0.001 003(19)	$\omega_e a_e$	0.000 030 4(28)		0.000 274(41)
B_e	1.820 046 5(53)	1.820 099(37)	1.820 053(11)	B_e	1.616 604 1(51)	1.616 627 5(24)	1.616 608(11)
$\alpha_e \times 10^3$	17.907 5(41)	18.012(63)	17.914 3(44)	$\alpha_e \times 10^3$	16.932 6(27)	16.969 1(51)	16.946 6(33)
$\gamma_e \times 10^3$	−0.136 8(23)	−0.063(29)	−0.088 6(17)	$\gamma_e \times 10^3$	−0.052 7(15)	−0.033 4(25)	−0.042 37(95)
$\delta_e \times 10^3$	−0.000 94(53)	−0.020 6(37)	−0.018 38(21)	$\delta_e \times 10^3$	0.001 42(32)	−0.001 54(33)	−0.000 629(81)
$\varepsilon_e \times 10^3$	−0.001 735(42)			$\varepsilon_e \times 10^3$	−0.000 119(21)		
$D_e \times 10^6$	6.972 4(19)	6.964(12)	6.952 6(66)	$D_e \times 10^6$	6.505 6(18)	6.508 6(54)	6.500 5(63)
$\beta_e \times 10^6$	0.034 4(11)	0.064 1(69)	0.067 5(12)	$\beta_e \times 10^6$	0.023 04(30)	0.025 3(29)	0.023 8(13)
$\zeta_e \times 10^6$	0.008 37(25)			$q \times 10^3$	−0.196 37(99)	−0.196 76(70)	−0.197 1(24)
				$\alpha^q \times 10^3$	0.001 62(24)	0.002 74(34)	0.001 34(54)[a]
				$q_D \times 10^6$	0.005 05(37)		0.006 1(16)
	$a^3\Pi_u$				$b^3\Sigma_g^-$		
	Present work	Amiot *et al.*[15]	Tanabashi *et al.*[28]		Present work	Amiot *et al.*[15]	Roux *et al.*[16]
T_e	720.008 3(21)	716.685 6(12)[b]		T_e	(6439.083 82(58))[c]	6435.736(21)	
				ΔT_e	5719.075 52(58)	(5719.050(21))[d]	5719.096 8(10)[e]
ω_e	1641.326 48(77)	1641.358 8(24)	1641.341(23)	ω_e	1470.365 02(68)	1470.415(13)	1470.374(7)
$\omega_e x_e$	11.649 04(36)	11.664 72(72)	11.658 0(58)	$\omega_e x_e$	11.135 54(35)	11.154 9(42)	11.143(3)
$\omega_e y_e$	−0.002 091(48)		−0.000 83(41)	$\omega_e y_e$	0.010 672 (69)	0.013 91(38)	0.012 8(4)
				$\omega_e z_e$	0.000 199 1(45)		
B_e	1.632 314 2(34)	1.632 532 3(36)	1.632 35(4)	B_e	1.498 664 7(34)	1.498 643 1(37)	1.498 64(5)
$\alpha_e \times 10^3$	16.541 7(13)	16.545 2(46)	16.57(3)	$\alpha_e \times 10^3$	16.287 47(58)	16.312 1(26)	16.29(3)
$\gamma_e \times 10^3$	−0.028 55(55)	−0.021 2(12)	−0.027(5)	$\gamma_e \times 10^3$	−0.011 02(16)	−0.004 61(38)	−0.009(5)
$\delta_e \times 10^3$	−0.000 918(68)			$\delta_e \times 10^3$	0.000 436(13)		
$D_e \times 10^6$	6.448 8(18)	6.437 5(20)	6.217 4(22)	$D_e \times 10^6$	6.221 0(18)	6.195 77(41)	6.200(8)
$\beta_e \times 10^6$	0.0147 1(30)	0.005 17(28)		$\beta_e \times 10^6$	0.011 15(14)	0.006 62(31)	−0.015(8)
$\zeta_e \times 10^6$	−0.000 861(87)	0.002 30(56)		$\zeta_e \times 10^6$	−0.000 267(26)	0.000 478(49)	
$H \times 10^{12}$	6.82(26)	2.916(69)	6.745(77)[f]	$H \times 10^{12}$	4.88(27)		2.3(9)
$\eta_e \times 10^{12}$		−0.631(63)					
A	−15.277 50(36)	−15.272 3(28)	−15.277 0(3)	A_{bX}	6.333 1(71)		5.65(38)[g]
α^A	0.016 51(13)	0.018 5(21)	0.016 0(4)	$A_{bXD} \times 10^3$	−0.043 3(28)		0.08(6)[g]
γ^A			0.000 36(7)				
$A_D \times 10^3$	0.234 4(23)	0.390 6(46)	0.238 8(33)[f]				
$\beta^{AD} \times 10^3$	−0.031 43(61)	−0.027 1(73)					
$\zeta^{AD} \times 10^3$		0.000 46(22)					
λ	−0.154 66(33)	−0.156 3(21)	−0.154 90(25)[f]	λ	0.158 89(23)	0.154 8(24)	0.152 9(18)
α^λ	0.000 30(12)	−0.003 38(84)		α^λ	−0.000 306(71)		−0.003 15(75)
$\lambda_D \times 10^3$	0.001 43(15)						
o	0.677 02(32)	0.678 1(18)	0.675 39(20)[f]	$\gamma \times 10^3$	−1.498(12)	−1.429(28)	−1.7(6)[f]
$\alpha^o \times 10^3$	−4.81(11)	−7.1(11)		$\alpha^\gamma \times 10^3$	−0.047 3(20)	−0.173(26)	
$o_D \times 10^3$	−0.002 44(16)		−0.787(58)[f]	$\delta^\gamma \times 10^3$		0.018 9(42)	
$p \times 10^3$	2.170(15)	4.25(37)	2.465(24)[f]	$\gamma_D \times 10^6$	0.021 5(27)		
$\alpha^p \times 10^3$	0.329 9(46)	0.56(24)					
$p_D \times 10^6$	−0.134 8(49)		0.063(14)[f]				
$q \times 10^3$	−0.500 0(12)	−1.020(13)	−0.531 9(20)[f]				
$\alpha^q \times 10^3$	−0.058 9(23)	−0.063(21)					
$\gamma^q \times 10^3$	0.005 8(12)						
$\delta^q \times 10^3$	−0.002 85(18)						
$q_D \times 10^6$	0.016 72(44)						

TABLE II. (*Continued.*)

	$a^3\Pi_u$			$b^3\Sigma_g^-$		
	Present work	Amiot *et al.*[15]	Tanabashi *et al.*[28]	Present work	Amiot *et al.*[15]	Roux *et al.*[16]
$\beta^{qD} \times 10^6$	0.007 0(10)					
$\zeta^{qD} \times 10^6$	−0.001 38(58)					
$\theta^{qD} \times 10^6$	0.000 551(95)					
$\sigma = 0.0037$ cm^{-1} for 6229 lines.						

[a]Corrected sign due to the different definition.
[b]Converted by 718.318 1(12) cm^{-1}–$B_e(a^3\Pi_u)$ with Brown and Merer's $^3\Pi$ Hamiltonian; see text for details.
[c]Derived value from $\Delta T_e(b^3\Sigma_g^- - a^3\Pi_u) + T_e(a^3\Pi_u)$.
[d]Derived value from $T_e(b^3\Sigma_g^-) - T_e(a^3\Pi_u)$.
[e]Converted by $\Delta T_0(b^3\Sigma_g^- - a^3\Pi_u) - G_0(b^3\Sigma_g^-) + G_0(a^3\Pi_u) + B_e(a^3\Pi_u)$, where $\Delta T_0(b^3\Sigma_g^- - a^3\Pi_u) = 5632.103\ 9(10)$ cm^{-1} and the molecular constants in $a^3\Pi_u$ were taken from Amiot *et al.*[15]
[f]Value of the effective constant in v = 0.
[g]Averaged value for different vibrational states. See text for details.

value:[15] our value is 721.64 cm^{-1} compared to Amiot *et al.*'s 718.32 cm^{-1} using Zare *et al.*'s definition, or 720.01 cm^{-1} versus Amiot *et al.*'s 716.69 cm^{-1} using Brown and Merer's definition. In both cases, our value of T_e is 3.32 cm^{-1} larger than that of Amiot *et al.*[15] It should be emphasized that both the N^2 and R^2 rotational Hamiltonians are effective Hamiltonians and, for example, the T_e values both include a $B\langle L^2\rangle$ contribution.

Since the energy difference ΔT_e ($b^3\Sigma_g^- - a^3\Pi_u$) is determined directly from the observed spectrum, the values of ΔT_e ($b^3\Sigma_g^- - a^3\Pi_u$) should be similar for different analyses (Amiot *et al.*,[15] Roux *et al.*,[16] and the present work) using the same definition of the Hamiltonian. Consequently, the values of T_e ($b^3\Sigma_g^-$) are also different, as shown in Table II.

The off diagonal spin-orbit interaction constant A_{bX} = 6.333(7) cm^{-1} between $b^3\Sigma_g^-$ and $X^1\Sigma_g^+$ is comparable with the average value of 5.7(4) cm^{-1} obtained from 5.05, 5.62, 6.03, and 5.90 cm^{-1}, which are converted from the previously determined spin-orbit interactions[15] $A_{bX}\langle v_b|v_X\rangle$ = 2.36(12), 2.73(6), 2.05(5), and 0.82(2) cm^{-1} and the present values of the vibrational overlap integrals $\langle v_b|v_X\rangle$ = 0.467, 0.486, 0.340, and 0.139 between the vibrational states v_b-v_X = 0-3, 1-4, 2-5, and 3-6, respectively, which are similar to the values of $\langle v_b|v_X\rangle$ calculated by Davis *et al.*[18]

Inclusion of several small molecular constants, γ^A and ζ^{AD} for $a^3\Pi_u$, and δ^γ for $b^3\Sigma_g^-$, in the least-squares fitting did not improve the overall standard deviation significantly and made other constants uncertain due to parameter correlation; they were set to zero in the final analysis. For the $a^3\Pi_u$ state up to v = 4, many higher-order expansions of the Λ-type doubling constants q_v and q_{Dv} with a slow convergence in the $(v + 1/2)^n$ dependence, as shown in Table II, are required for the fit even when we remove the bands associated with v = 4 of $a^3\Pi_u$, which may indicate that there are some small perturbations from other states, probably v = 0 of the $c^3\Sigma_u^+$ state as seen in Fig. 1. The v = 5 and 6 of $a^3\Pi_u$ bracket v = 0 of $c^3\Sigma_u^+$ in energy, and much more prominent perturbations with opposite directions for the frequency shifts for the bands associated with v = 5 and 6 of $a^3\Pi_u$, as shown in the supplementary material,[23] may be explained by the interactions among the three states, which will be discussed in a future paper.

IV. LEVEL CROSSINGS FOR POTENTIAL FORBIDDEN TRANSITIONS

By setting the spin-orbit interaction constants A_{bX} and A_{bXD} to zero, we can calculate the frequency shifts due to the spin-orbit interaction, i.e., the magnitude of the perturbation. In Table III, we list the lines with perturbations larger than 0.1 cm^{-1}. These perturbed lines were all known from previous studies[15] except for the lines involved with the energy level crossing at J = 2 for v = 3(F_1) of $b^3\Sigma_g^-$ and v = 6 of $X^1\Sigma_g^+$ (Fig. 2), which was thought previously to have a crossing only at $J < 0$ (in other words, not strongly perturbed). For example, the assigned transition for J = 3-2 and v = 4-6 of the Phillips system by Douay *et al.*[19] showed no perturbation.

With the calculation in the present analysis, the energy difference at J = 2 between v = 3(F_1) of $b^3\Sigma_g^-$ and v = 6 of $X^1\Sigma_g^+$ is only 0.07 cm^{-1} without considering the spin-orbit interaction, and the two energy levels are shifted apart by about ±0.5 cm^{-1} with the 0.89 cm^{-1} spin-orbit interaction. This nearly degenerate perturbation makes the wave functions of the singlet and triplet states mix almost completely, which should result in the corresponding forbidden transitions having

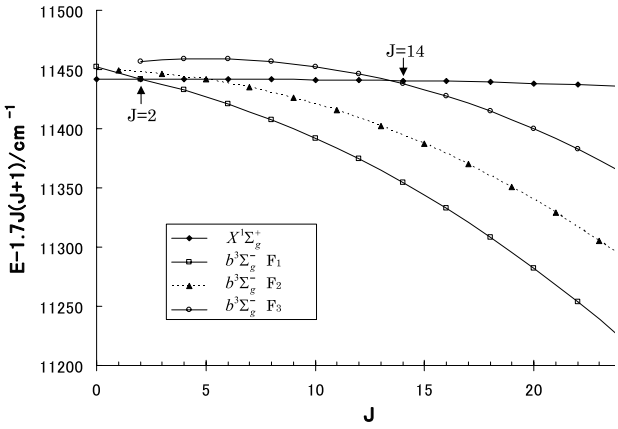

FIG. 2. Plot of the calculated term energies of $X^1\Sigma_g^+$ (v = 6) and $b^3\Sigma_g^-$ (v = 3) vs. rotational quantum number J. The term energies have $1.7J(J+1)$ subtracted to make the $X^1\Sigma_g^+$ (v = 6) curve close to a horizontal line. The level crossing occurs at J = 2 of $b^3\Sigma_g^-$ v = 3 (F_1) and at J = 14 of $b^3\Sigma_g^-$ v = 3 (F_3) with $X^1\Sigma_g^+$ v = 6.

TABLE III. C_2 transitions with perturbations larger than 0.1 cm^{-1}.

v′-v″	$J'-J''$	Observed	O-C	Δ[a]
Phillips system $A^1\Pi_u$–$X^1\Sigma_g^+$				
3-6	2-2	2429.5949	−0.0041	0.5495
4-6	2-2	3940.7094	−0.0017	0.5495
6-6	2-2	6889.5784	−0.0067	0.5495
7-6	3-2	8336.0974	0.0019	0.5495
3-6	14-14	2400.8452	−0.0042	−0.1560
3-6	15-14	2447.4118	−0.0081	−0.1560
4-6	14-14	3908.4271	−0.0006	−0.1560
4-6	15-14	3954.4797	0.0009	−0.1560
6-6	13-14	6808.0851	0.0000	−0.1560
6-6	14-14	6850.1767	0.0026	−0.1560
6-6	15-14	6895.1820	0.0045	−0.1560
7-6	14-14	8284.1660	−0.0028	−0.1560
7-6	15-14	8328.6551	0.0116	−0.1560
3-5	25-26	3912.0813	−0.0023	0.1147
3-5	26-26	3992.6941	−0.0034	0.1147
3-5	27-26	4076.1067	0.0003	0.1147
5-5	25-26	6887.4992	−0.0025	0.1147
5-5	26-26	6966.2952	−0.0090	0.1147
3-5	27-28	3888.3297	−0.0070	−0.1659
3-5	28-28	3975.0886	0.0065	−0.1659
3-5	29-28	4064.5799	0.0064	−0.1659
5-5	27-28	6860.0658	−0.0009	−0.1659
5-5	28-28	6944.8633	0.0026	−0.1659
Ballik-Ramsay system $b^3\Sigma_g^-$–$a^3\Pi_u$				
3-1	$2(F_1)$-$2(F_1)$	8306.8935	−0.0012	0.5182
3-1	$2(F_1)$-$2(F_2)$	8284.8733	0.0029	0.5182
3-1	$2(F_1)$-$2(F_3)$	8266.5251	0.0027	0.5182
3-1	$2(F_1)$-$3(F_1)$	8298.6003	0.0059	0.5182
3-2	$2(F_1)$-$2(F_1)$	6712.2278	0.0035	0.5182
3-2	$2(F_1)$-$2(F_2)$	6690.2845	0.0020	0.5182
3-2	$2(F_1)$-$3(F_1)$	6704.0040	0.0019	0.5182
3-2	$2(F_1)$-$3(F_2)$	6681.2569	−0.0005	0.5182
3-2	$2(F_1)$-$3(F_3)$	6661.9459	−0.0035	0.5182
3-4	$2(F_1)$-$1(F_2)$	3577.1428	0.0046	0.5182
3-4	$2(F_1)$-$2(F_1)$	3592.8853	−0.0001	0.5182
3-4	$2(F_1)$-$2(F_2)$	3571.1089	−0.0005	0.5182
3-4	$2(F_1)$-$2(F_3)$	3552.9740	0.0022	0.5182
3-4	$2(F_1)$-$3(F_1)$	3584.8143	−0.0061	0.5182
3-4	$2(F_1)$-$3(F_2)$	3562.2679	0.0033	0.5182
3-1	$14(F_3)$-$13(F_3)$	8298.6003	−0.0037	−0.1504
3-1	$14(F_3)$-$14(F_3)$	8250.1384	−0.0015	−0.1504
3-1	$14(F_3)$-$15(F_3)$	8199.4993	−0.0014	−0.1504
3-2	$14(F_3)$-$13(F_3)$	6707.3763	−0.0002	−0.1504
3-2	$14(F_3)$-$13(F_2)$	6755.0469	−0.0042	−0.1504
3-2	$14(F_3)$-$14(F_3)$	6659.4285	0.0056	−0.1504
3-2	$14(F_3)$-$14(F_2)$	6709.9675	0.0048	−0.1504
3-2	$14(F_3)$-$15(F_3)$	6609.3071	0.0007	−0.1504
3-4	$14(F_3)$-$13(F_3)$	3594.9584	0.0021	−0.1504
3-4	$14(F_3)$-$14(F_3)$	3548.0474	−0.0044	−0.1504
3-4	$14(F_3)$-$14(F_2)$	3597.5869	0.0019	−0.1504
3-4	$14(F_3)$-$15(F_3)$	3498.9619	−0.0012	−0.1504
2-0	$26(F_1)$-$25(F_1)$	8482.6245	−0.0066	0.1020
2-0	$26(F_1)$-$26(F_1)$	8401.8962	−0.0018	0.1020
2-0	$26(F_1)$-$27(F_1)$	8317.6552	−0.0039	0.1020
2-3	$26(F_1)$-$25(F_1)$	3728.5148	−0.0041	0.1020
2-3	$26(F_1)$-$26(F_1)$	3650.4388	−0.0017	0.1020
2-3	$26(F_1)$-$27(F_1)$	3568.6399	−0.0001	0.1020
2-0	$28(F_1)$-$28(F_1)$	8383.9151	0.0019	−0.1806
2-0	$28(F_1)$-$29(F_1)$	8293.2485	−0.0014	−0.1806
2-1	$28(F_1)$-$27(F_1)$	6864.6108	0.0005	−0.1806
2-1	$28(F_1)$-$28(F_1)$	6778.4871	−0.0013	−0.1806
2-1	$28(F_1)$-$28(F_2)$	6686.5916	−0.0029	−0.1806
2-1	$28(F_1)$-$29(F_1)$	6688.7066	−0.0001	−0.1806
2-3	$28(F_1)$-$27(F_1)$	3721.9621	0.0027	−0.1806
2-3	$28(F_1)$-$28(F_1)$	3637.7738	0.0023	−0.1806
2-3	$28(F_1)$-$29(F_1)$	3549.7230	−0.0020	−0.1806
2-0	$38(F_3)$-$37(F_3)$	8373.0540	0.0083	0.2140
2-0	$38(F_3)$-$38(F_3)$	8248.1563	0.0032	0.2140
2-0	$38(F_3)$-$39(F_3)$	8119.6537	0.0001	0.2140
2-1	$38(F_3)$-$37(F_3)$	6779.6173	0.0028	0.2140
2-1	$38(F_3)$-$38(F_3)$	6656.0851	0.0069	0.2140
2-1	$38(F_3)$-$39(F_3)$	6528.8549	0.0056	0.2140
2-3	$38(F_3)$-$38(F_3)$	3542.2290	0.0030	0.2140
1-0	$40(F_1)$-$39(F_1)$	6974.9013	−0.0115	0.2668
1-0	$40(F_1)$-$40(F_1)$	6850.2925	−0.0075	0.2668
1-0	$40(F_1)$-$41(F_1)$	6721.3755	−0.0132	0.2668
1-1	$40(F_1)$-$39(F_1)$	5381.4870	−0.0093	0.2668
1-1	$40(F_1)$-$40(F_1)$	5258.2536	−0.0111	0.2668
1-1	$40(F_1)$-$41(F_1)$	5130.5887	−0.0096	0.2668
1-2	$40(F_1)$-$41(F_1)$	3563.2200	0.0007	0.2668
1-0	$42(F_1)$-$41(F_1)$	6956.4969	0.0043	−0.1383
1-0	$42(F_1)$-$42(F_1)$	6825.7155	0.0077	−0.1383
1-0	$42(F_1)$-$43(F_1)$	6690.4903	0.0033	−0.1383
1-1	$42(F_1)$-$41(F_1)$	5365.7093	0.0071	−0.1383
1-1	$42(F_1)$-$42(F_1)$	5236.3747	0.0014	−0.1383
1-1	$42(F_1)$-$43(F_1)$	5102.4622	0.0055	−0.1383
1-2	$42(F_1)$-$42(F_1)$	3670.4712	−0.0010	−0.1383
1-2	$42(F_1)$-$43(F_1)$	3537.8549	0.0078	−0.1383
0-0	$50(F_1)$-$49(F_1)$	5464.5519	−0.0054	0.1141
0-0	$50(F_1)$-$50(F_1)$	5309.3696	−0.0018	0.1141
0-0	$50(F_1)$-$51(F_1)$	5149.1484	−0.0054	0.1141
0-0	$52(F_1)$-$51(F_1)$	5443.5669	0.0049	−0.1614
0-0	$52(F_1)$-$52(F_1)$	5282.3570	0.0043	−0.1614
0-0	$52(F_1)$-$53(F_1)$	5115.9535	−0.0001	−0.1614
Forbidden transitions $A^1\Pi_u$–$b^3\Sigma_g^-$				
4-3	$2-2(F_1)$	3939.5614	−0.0041	−0.5182
Forbidden transitions $X^1\Sigma_g^+$–$a^3\Pi_u$				
6-1	$2-1(F_2)$	8289.9426	−0.0008	−0.5495
6-1	$2-2(F_1)$	8305.7451	−0.0040	−0.5495
6-1	$2-3(F_1)$	8297.4453	−0.0035	−0.5495
6-2	$2-2(F_1)$	6711.0706	−0.0081	−0.5495
6-2	$2-2(F_2)$	6689.1333	−0.0035	−0.5495
6-2	$2-3(F_1)$	6702.8449	−0.0116	−0.5495
6-4	$2-2(F_1)$	3591.7409	0.0011	−0.5495
6-4	$2-2(F_2)$	3569.9558	−0.0080	−0.5495
6-4	$2-3(F_1)$	3583.6837	0.0089	−0.5495
6-1	$14-14(F_3)$	8253.0015	0.0053	0.1560
6-1	$14-15(F_3)$	8202.3585	0.0015	0.1560

TABLE III. (*Continued.*)

v′-v″	$J'-J''$	Observed	O-C	Δ[a]	v′-v″	$J'-J''$	Observed	O-C	Δ[a]
Ballik-Ramsay system $b^3\Sigma_g^- - a^3\Pi_u$					Forbidden transitions $X^1\Sigma_g^+ - a^3\Pi_u$				
2-1	26(F_1)-25(F_1)	6874.5727	0.0018	0.1020	6-2	14-14(F_3)	6662.2830	0.0038	0.1560
2-1	26(F_1)-26(F_1)	6794.7030	−0.0060	0.1020	6-2	14-15(F_3)	6612.1625	−0.0002	0.1560
2-1	26(F_1)-26(F_2)	6709.0289	−0.0019	0.1020	6-4	14-13(F_3)	3597.8123	−0.0003	0.1560
2-1	26(F_1)-27(F_1)	6711.2885	−0.0023	0.1020	6-4	14-14(F_3)	3550.9110	0.0029	0.1560
2-2	26(F_1)-27(F_1)	5128.2777	−0.0030	0.1020					

[a]Frequency shift due to the spin-orbit interaction between the $X^1\Sigma_g^+$ and $b^3\Sigma_g^-$ states.

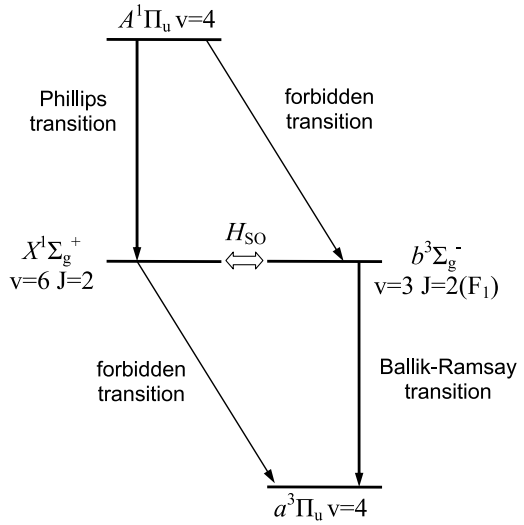

FIG. 3. Forbidden transitions due to the energy level crossing. The upper forbidden transition is associated with the allowed transition of the Phillips system, and the lower forbidden transition is associated with the allowed transition of the Ballik-Ramsay system.

similar intensities to the allowed ones. According to the deperturbation analysis, at the level crossing for $J = 2$, the mixed wave functions have a 57% contribution from the parent state and a 43% contribution from the perturber. Therefore, the intensity borrowing from the allowed transition makes the forbidden transition in Fig. 3 have an intensity ratio of 43%:57% = 0.75.

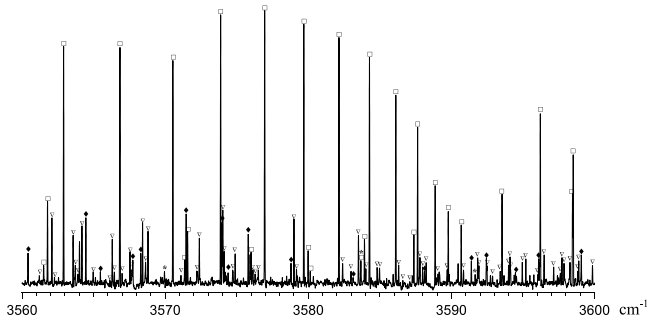

FIG. 4. A portion of the Fourier transform emission spectrum taken from Ref. 21. The strong lines marked with □ belong to the v = 0-0 band of the $B^1\Delta_g - A^1\Pi_u$ system (Ref. 12). The lines marked with ∇ belong to the v = 3-4 band of the Ballik-Ramsay $b^3\Sigma_g^- - a^3\Pi_u$ system assigned in the present study. The lines marked with ♦ belong to the v = 2-4 and 3-5 bands of the $B'^1\Sigma_g^+ - A^1\Pi_u$ system. The three lines marked with * are forbidden transitions assigned in the present study.

For v = 3(F_3) of $b^3\Sigma_g^-$ and v = 6 of $X^1\Sigma_g^+$, a level crossing at $J = 14$ was known previously (Fig. 2), which has a 2.75 cm^{-1} energy difference without considering the spin-orbit interaction. Our deperturbation analysis showed that the same 0.89 cm^{-1} spin-orbit interaction makes the energy levels shift apart by about ±0.15 cm^{-1}, and the intensity borrowing from the allowed transitions makes the forbidden transitions have an intensity ratio of 0.06.

The level crossing at $J = 52$ for v = 1(F_3) of $b^3\Sigma_g^-$ and v = 4 of $X^1\Sigma_g^+$ has a 1.45 cm^{-1} energy difference without considering the spin-orbit interaction, and the levels are shifted apart by about ±1.5 cm^{-1} with the 3.06 cm^{-1} spin-orbit interaction. According to the deperturbation analysis on this level crossing, the wave functions are a 75%:25% mixture,

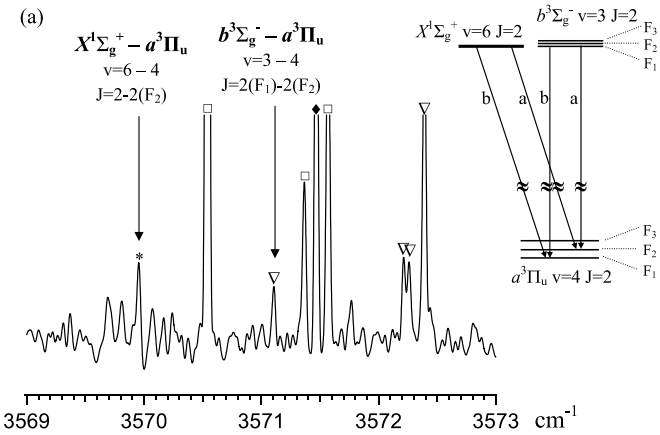

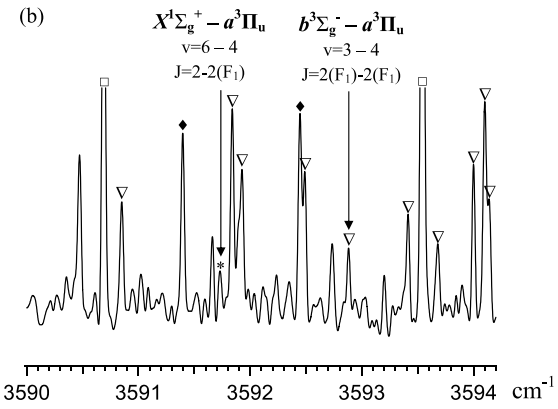

FIG. 5. Two short sections of spectra, (a) and (b), that show forbidden transitions and corresponding allowed transitions. The symbols have the same meaning as in Fig. 4.

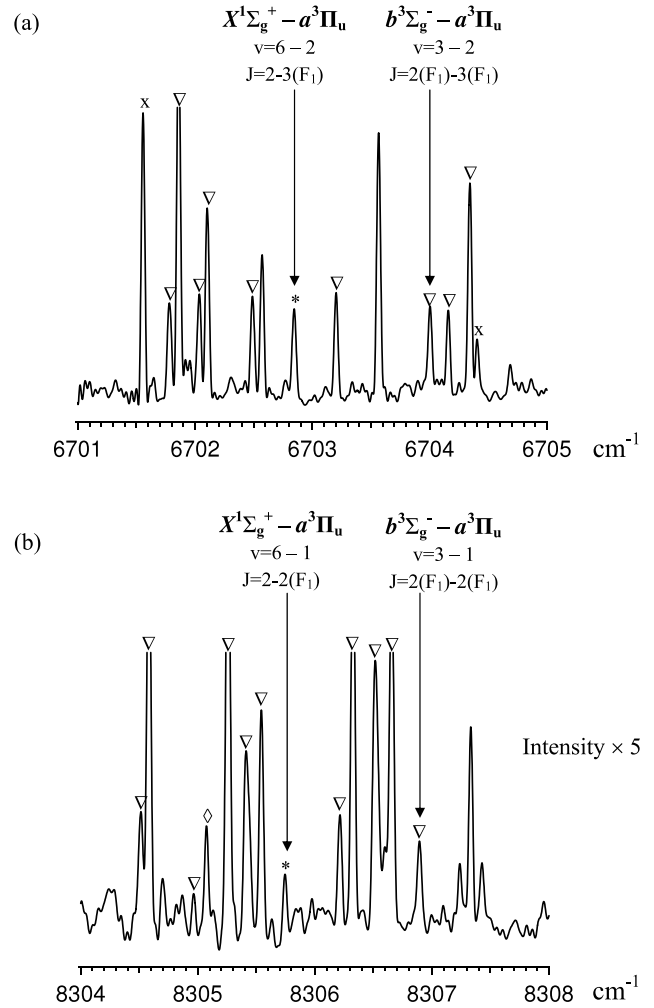

FIG. 6. More forbidden transitions and corresponding allowed transitions. The intensity scale in (b) has been magnified by five times relative to the intensity scale in (a). The lines marked with x belong to the $A^2\Pi$–$X^2\Sigma^+$ transitions of the carbon phosphide (CP) radical (Ref. 30).

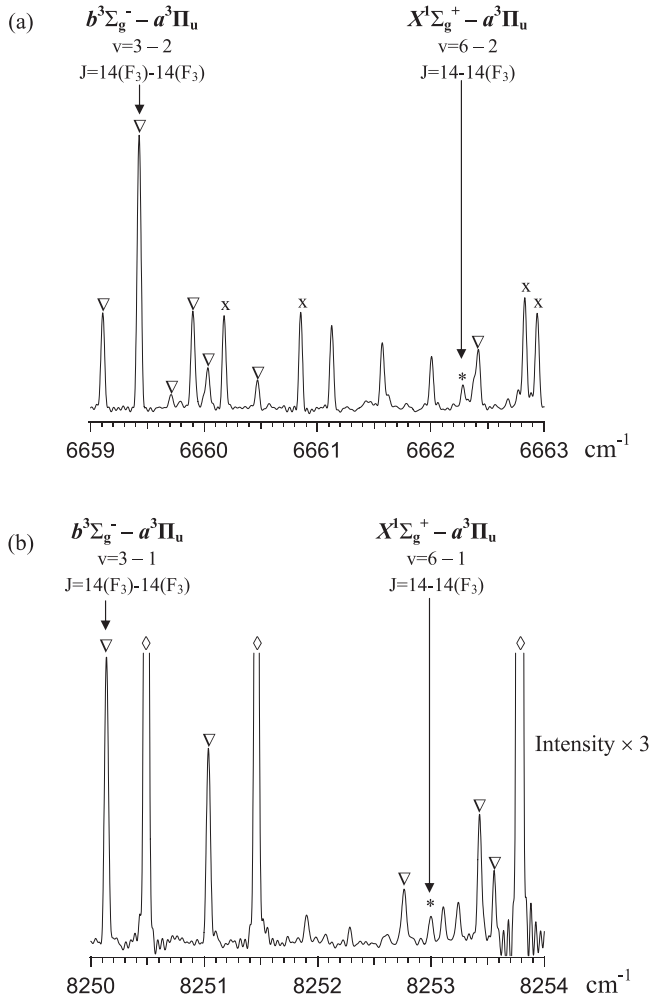

FIG. 7. Additional forbidden transitions and corresponding allowed transitions. The intensity scale in (b) has been magnified by three times relative to the intensity scale in (a). The lines marked with ◊ belong to the Phillips $A^1\Pi_u$–$X^1\Sigma_g^+$ system.

which leads to an intensity ratio of 0.33 for the forbidden to the allowed transitions. However, the assignment for J = 52-52(F$_3$) of v = 1-0 and 1-1 bands in the Ballik-Ramsay system by Roux *et al.*[16] showed a perturbation shift of 1.0 cm^{-1}, which is inconsistent with our calculated shift of 1.5 cm^{-1} (see the supplementary material[23]) and is an erroneous assignment.

V. ASSIGNMENT OF THE FORBIDDEN TRANSITIONS

In Sec. II, we have assigned several bands of the Ballik-Ramsay system by using a Fourier transform emission spectrum in the range of 1800-4000 cm^{-1} with a spectral resolution of 0.02 cm^{-1} taken previously with the discharge of a CH_4 and He mixture for the study of the CH radical.[21] A small portion of the spectrum (Fig. 4) shows the strong v = 0-0 band of the $B^1\Delta_g$–$A^1\Pi_u$ system[12] and the new v = 3-4 band of the Ballik-Ramsay system and the weak v = 2-4 and 3-5 bands of the $B'^1\Sigma_g^+$–$A^1\Pi_u$ system, which will be presented in another publication. In the spectrum, three forbidden transitions between v = 6 of $X^1\Sigma_g^+$ and v = 4 of $a^3\Pi_u$ were found at 3569.956, 3583.684, and 3591.741 cm^{-1}. The forbidden transition at 3569.956 cm^{-1} with J = 2-2 for v = 6 of $X^1\Sigma_g^+$ and v = 4(F$_2$) of $a^3\Pi_u$ corresponds to the allowed transition at 3571.109 cm^{-1} for J = 2-2 for v = 3(F$_1$) of $b^3\Sigma_g^-$ and v = 4(F$_2$) of $a^3\Pi_u$, and is due to the strong upper-level mixing between v = 6 of $X^1\Sigma_g^+$ and v = 3(F$_1$) of $b^3\Sigma_g^-$. This pair of allowed and forbidden transitions shows comparable intensity (Fig. 5(a)) as predicted in Sec. IV, and the wavenumber of the forbidden transition is also consistent with the prediction to within 0.02 cm^{-1}, which was reduced further to less than 0.01 cm^{-1} by adding this transition to the least-squares fit. Also, the forbidden transition at 3591.741 cm^{-1} (Fig. 5(b)) with J = 2-2 for v = 6 of $X^1\Sigma_g^+$ and v = 4(F$_1$) of $a^3\Pi_u$ was assigned within the predicted wavenumber range: the line is slightly weaker than the corresponding allowed transition at 3592.885 cm^{-1} with J = 2-2 for v = 3(F$_1$) of $b^3\Sigma_g^-$ and v = 4(F$_1$) of $a^3\Pi_u$. By checking in the v = 3-2 and 3-1 bands of the Ballik-Ramsay system in the spectrum of Ref. 19, six more forbidden transitions were assigned as listed in Table III and two of them are shown in Fig. 6.

At the level crossing at J = 14 for v = 3(F$_3$) of $b^3\Sigma_g^-$ and v = 6 of $X^1\Sigma_g^+$, six forbidden transitions for v = 6-1(F$_3$), 6-2(F$_3$), and 6-4(F$_3$) between $X^1\Sigma_g^+$ and $a^3\Pi_u$ were assigned

as listed in Table III and the observed intensity ratios to the corresponding allowed transitions are about 10%, which are comparable to the predicted 6% intensity ratio. Fig. 7 shows two of the forbidden transitions and the corresponding allowed transitions.

We also searched for forbidden transitions between $A^1\Pi_u$ and $b^3\Sigma_g^-$ corresponding to the allowed transitions of the Phillips system. However, due to the weak intensity of the forbidden transitions at the level crossing and the accidental disturbance by nearby strong transitions, only one such forbidden transition was identified as listed in Table III.

The forbidden and allowed transitions involved in the level crossing at $J = 52$ for v = 1 (F_3) of $b^3\Sigma_g^-$ and v = 4 of $X^1\Sigma_g^+$ could not be assigned because only transitions with a maximum J value of about 37 were observed in our Fourier transform emission spectra.

VI. CONCLUSIONS

A deperturbation analysis using 6229 transitions of the Ballik-Ramsay system and the Phillips system of C_2 led to the determination of the energy difference between the $X^1\Sigma_g^+$ and $a^3\Pi_u$ states as 720.008(2) cm^{-1}, which is about 3.3 cm^{-1} larger than the previous value. A new energy-level crossing was found at $J = 2$ between v = 3 of $b^3\Sigma_g^-$ and v = 6 of $X^1\Sigma_g^+$, where the strong spin-orbit interaction causes a nearly complete mixing between the wave functions of the $b^3\Sigma_g^-$ and $X^1\Sigma_g^+$ states and forbidden transitions between the $X^1\Sigma_g^+$ and $a^3\Pi_u$ states were found with similar intensity as the corresponding allowed transitions. The observation of the forbidden transitions at the predicted line positions and intensities verifies the new value of the energy difference between the $X^1\Sigma_g^+$ and $a^3\Pi_u$ states. Recently, the deperturbation of the $c^3\Sigma_u^+$, $a^3\Pi_u$, and $A^1\Pi_u$ states by Nakajima and Endo[10] also required the singlet-triplet energy gap to be increased by about 3 cm^{-1} from the literature value,[15] which is consistent with our results.

ACKNOWLEDGMENTS

The present study was partially supported by the Grant-in-Aid (Grant No. 21104003) from the Ministry of Education, Culture, Sports, Science and Technology of Japan. Some support was also provided by the NASA laboratory astrophysics program.

[1]J. S. A. Brooke, P. F. Bernath, T. W. Schmidt, and G. B. Bacskay, J. Quant. Spectrosc. Radiat. Transfer **124**, 11 (2013).
[2]M. Martin, J. Photochem. Photobiol., A **66**, 263 (1992).
[3]E. A. Ballik and D. A. Ramsay, J. Chem. Phys. **31**, 1128 (1959).
[4]E. A. Ballik and D. A. Ramsay, Astrophys. J. **137**, 61 (1963).
[5]E. A. Ballik and D. A. Ramsay, Astrophys. J. **137**, 84 (1963).
[6]J. Chauville, J. P. Maillard, and A. W. Mantz, J. Mol. Spectrosc. **68**, 399 (1977).
[7]S. P. Davis, M. C. Abrams, J. G. Phillips, and M. L. P. Rao, J. Opt. Soc. Am. B **5**, 2280 (1988).
[8]D. L. Kokkin, N. J. Reilly, C. M. Morris, M. Nakajima, K. Nauta, S. H. Kable, and T. W. Schmidt, J. Chem. Phys. **125**, 231101 (2006).
[9]T. W. Schmidt, "Astronomical molecular spectroscopy," in *Computational Spectroscopy: Methods, Experiments and Applications*, edited by J. Grunenberg (Wiley, Weinheim, 2010), p. 386.
[10]M. Nakajima and Y. Endo, J. Mol. Spectrosc. **302**, 9 (2014); **305**, 48 (2014).
[11]J. G. Phillips, J. Mol. Spectrosc. **28**, 233 (1968).
[12]M. Douay, R. Nietmann, and P. F. Bernath, J. Mol. Spectrosc. **131**, 261 (1988).
[13]K. Kirby and B. Liu, J. Chem. Phys. **70**, 893 (1979).
[14]P. Bornhauser, Y. Sych, G. Knopp, T. Gerber, and P. P. Radi, J. Chem. Phys. **134**, 044302 (2011).
[15]C. Amiot, J. Chauville, and J. P. Maillard, J. Mol. Spectrosc. **75**, 19 (1979).
[16]F. Roux, G. Wannous, F. Michaud, and J. Verges, J. Mol. Spectrosc. **109**, 334 (1985).
[17]E. Kagi and K. Kawaguchi, J. Mol. Struct. **795**, 179 (2006).
[18]S. P. Davis, M. C. Abrams, Sandalphon, J. W. Brault, and M. L. P. Rao, J. Opt. Soc. Am. B **5**, 1838 (1988).
[19]M. Douay, R. Nietmann, and P. F. Bernath, J. Mol. Spectrosc. **131**, 250 (1988).
[20]M.-C. Chan, S.-H. Yeung, Y.-Y. Wong, Y. Li, W.-M. Chan, and K.-H. Yim, Chem. Phys. Lett. **390**, 340 (2004); S.-H. Yeung, Ph.D. thesis, The Chinese University of Hong Kong, Hong Kong, 2009.
[21]P. N. Ghosh, M. N. Deo, and K. Kawaguchi, Astrophys. J. **525**, 539 (1999).
[22]W.-B. Yan, R. F. Curl, A. J. Merer, and P. G. Carrick, J. Mol. Spectrosc. **112**, 436 (1985).
[23]See supplementary material at http://dx.doi.org/10.1063/1.4907530 for the total line list used in the present analysis.
[24]J. M. Brown and A. J. Merer, J. Mol. Spectrosc. **74**, 488 (1979).
[25]C. R. Brazier, R. S. Ram, and P. F. Bernath, J. Mol. Spectrosc. **120**, 381 (1986).
[26]R. J. Le Roy, LEVEL 7.7: A Computer Program for Solving the Radial Schrödinger Equation for Bound and Quasibound Levels, University of Waterloo Chemical Physics Research Report CP-661, 2005, see http://leroy.uwaterloo.ca/programs/.
[27]R. N. Zare, A. L. Schmeltekopf, W. J. Harrop, and D. L. Albritton, J. Mol. Spectrosc. **46**, 37 (1973).
[28]A. Tanabashi, T. Hirao, T. Amano, and P. F. Bernath, Astrophys. J., Suppl. Ser. **169**, 472 (2007).
[29]M. Nakajima and Y. Endo, J. Chem. Phys. **139**, 244310 (2013).
[30]R. S. Ram, J. S. A. Brooke, C. M. Western, and P. F. Bernath, J. Quant. Spectrosc. Radiat. Transfer **138**, 107 (2014).